ORIGINAL PAPER

Electrochemical impedance and cyclic voltammetry analysis of PEDOT: PSS-AgNPs composites

Shadab Anwar Khan[1] · Sandhya Patel[1] · Prashant Shukla[1]

Abstract

Conducting polymer PEDOT:PSS was mixed with Silver nanoparticles synthesised using green method. Nanocomposites were prepared through chemical deposition method, and their potential in optoelectronic and charge storage applications is explored. Structural properties of the nanocomposite were investigated using SEM and XRD. Electrodes made with AgNPs-PEDOT:PSS nanocomposite was investigated to analyse the specific capacitance, constant phase element, electrical, and ionic conductivity by EIS. Capacitive properties were further explored by Cyclic voltammetry where a sudden increase in specific capacitance was observed with the increasing amount of Silver nanoparticles into the matrix of PEDOT:PSS. Capacitance for AgNPs-deposited pellets increases especially for AgNPs-PEDOT:PSS 15% which illustrates the formation of the metal-polymer layer that stores the charges.

Introduction

Conducting polymers have a very special place in the class of polymers thanks to their properties to conduct electricity. Their conductivity falls in between the conductivity of metals and semiconductors. Poly(pyrrole) [1], polyanilines (PANI) [2], and Poly(3,4-ethylenedioxythiophene):Poly(styrene sulfonate) PEDOT: PSS [3], are some of the better known conducting polymers. Combination of (PEDOT:PSS) is a widely used polymer that is used as an electrolyte solution as well as a flexible electrode in a variety of electrical applications, particularly optoelectronic devices, such as solar cells and light-emitting diodes (LED) [4]. In solar cells, it acts as a "hole transfer layer" and in LEDs, it acts as a "hole junction layer". In organic solar cells, it works as the "hole transferring layer" between the active organic layer and the anode. PEDOT:PSS is a much less expensive option in comparison with other conducting polymers, like PANI (Polyaniline). Similarly silver nitrate is much more cost-friendly than the precursor used to make gold nanoparticles; Aurochloric acid and silicon which is normally used for these photovoltaic purposes, making this procedure very cost effective and reproducible.

Nanoparticles exhibit surface plasmon resonance in a near-visible region. Particles that show the property of surface plasmon resonance are called surface plasmons. Surface plasmons produce waves by coupling between incident electromagnetic radiation and electrons from the metal's conduction band when the frequency of the incident radiation is equal to the frequency of surface plasmon resonance. This effect leads to a major electromagnetic field around nanoparticles, which makes the absorption of light grow higher. It can also improve the light scattering potential of the photoactive layer, enhancing its ability to trap light. Since all these special properties of silver nanoparticles depend on localised surface plasmon resonance (LSPR) and LSPR depends upon the size of nanoparticles, these properties become tunable with the size of the Silver nanoparticles (AgNPs). These optical properties can be controlled by tuning the size of nanoparticles which can be valuable for building a well-operational photovoltaic device.

Thin films of PEDOT:PSS are typically created by dispersing PEDOT in water and forming a non-stoichiometric combination with PSS. Even though PEDOT by itself has excellent conductivity, the complexation with PSS tends to weaken that conductivity. Silver nanoparticles are therefore introduced to the conducting polymer (PEDOT:PSS) to improve its conductivity. The PEDOT:PSS polymer's conductivity is improved by the addition of silver nanoparticles, yet the processability of the resulting nanocomposites is also maintained.

✉ Shadab Anwar Khan
shadabanwar11@gmail.com

1   Dr. HariSingh Gour Vishwavidyalaya, Sagar, M.P., India

In this paper, we present an ex situ technique for preparing silver nanoparticle polymer by dispersing nanoparticles in a water bath as in chemical solution deposition method and then mixing this composite with PEDOT: PSS solution. Due to the low cost, stability and adjustable conductivity of PEDOT:PSS and the easy to fabricate procedure of green-synthesised silver nanoparticles there is a significant prospect for the scaling up of the sample [5]. Even though there has been literature on the effect of silver nanoparticles on a conducting polymer like PEDOT:PSS, an extensive electrochemical and optical study of these nanocomposites is yet to be explored. In this work, we explain how the incorporation of AgNPs modifies the dielectric constant and the conductivity of PEDOT: PSS and report that these composites show electronic double-layer behaviour more extensively than the pure PDS pellets. We study how different concentrations of AgNPs affect the optical band gap of these films and the structure of nanocomposites, exploring new horizons in their optoelectronic applications.

Experimental methodology

Silver nanoparticles have been synthesised using clove extract using the Green method, which we reported in our previous work [6]. Afterwards, 0.15 g of 4% PEDOT:PSS (PDS) solution is added with 0.076-g AgNPs solution to make the 5% AgNPs-PDS solution. Moreover, 10% solution was prepared by adding 0.118-g AgNPs were mixed with 0.2308-g PEDOT:PSS. And finally 0.383-g PEDOT:PSS is mixed with 0.084-g AgNPs to make 15% AgNPs-PDS solution. 1 ml of each concentration was placed on a magnetic stirrer at 500 rpm at a temperature of 50 °C for 3 h. In the end, Pure PEDOT:PSS sample was prepared with 0.767 g of PEDOT:PSS. These mixtures of nanocomposites were stored at 4 °C for further characterisation. To prepare electrodes using nanocomposites, solution was dried by heating in a vacuum oven for 6 h at 70 °C; moreover, the dried sample was beaten into a fine powder using a mortar pestle.

For Cyclic voltammetry, slurry of nanocomposites in DI water was prepared which was coated on a steel sheet of 2cm² to make an electrode using a fine brush. Afterwards, the steel sheet electrode was annealed at 80 °C for 15 min. Finally, for (EIS) Electrochemical Impedance Spectroscopy, pellets of 1 cm diameter were prepared. To prepare these pellets Silver nanoparticles with PEDOT:PSS nanocomposites were ground well in a mortar pestle and then their pellets of 0.5 mm thickness were prepared under the hydraulic press for 5 min at 500 kg/cm². In the end, those pellets were annealed at 70 °C for 20 min and then a coating of Silver paste was applied on each surface of the pellets for the EIS characterization.

Results and discussion

SEM (scanning electron microscopy)

A careful look at the SEM images reveals that the synthesised nanocomposites are oblate, tetragons, and ellipsoidal in shape as shown in Fig. 1. This figure shows the as-prepared nanocomposites at the magnification of 1 μm to 500 nm where nanocomposites with sub-100 nm size are visible in these images. Coagulation of nanocomposites of around 2–7-μm agglomerates is detected in Fig. 1b, c, and d.

Presence of metallic Silver from Silver nanoparticles, Sulphur, and Carbon from PEDOT:PSS was confirmed through Energy-dispersive X-ray spectroscopy (EDX) analysis [7] and their concentration is displayed in Fig. 1 given in supplemental material.
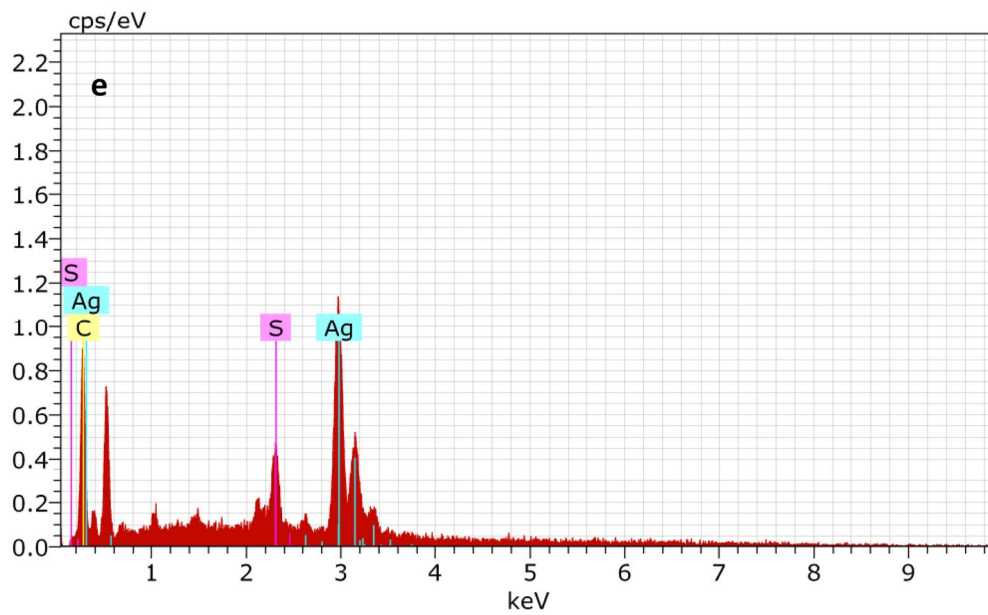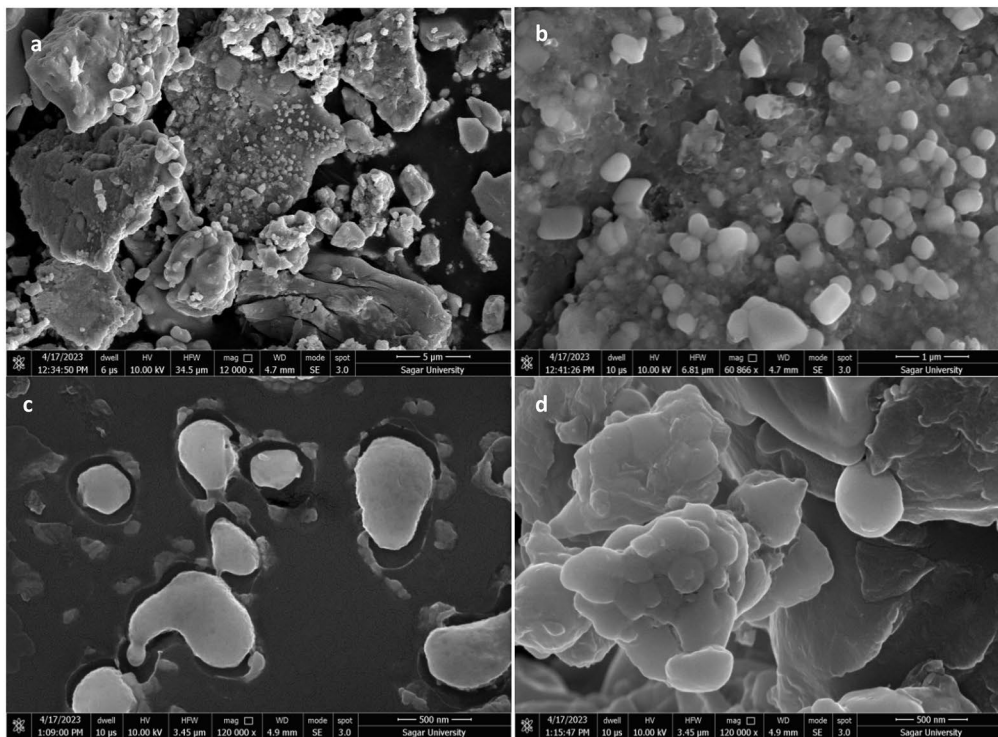
XRD

X-ray diffraction characterisation was done to obtain the comparative structural results of pure PDS (PEDOT:PSS) with AgNPs at various proportions. It gives us the structure and phase purity of our sample. In the graph, we can see the amorphous nature of the polymer PEDOT:PSS, whereas the involvement of Silver nanoparticles increases the extent of crystallinity of the graphs. Characteristic peak at 38° for FCC (111) planes of Ag is observed which signifies the presence of AgNPs in all the composite samples (JCPDS 04-0783). We can see that as the amount of Silver nanoparticles is increased the number of Ag peaks visible in the graph has also increased. In the case of AgNPs-PEDOT:PSS 15% peaks for 2θ = 44°, 68°, and 77° are also visible that correspond to the plane (200), (220), and (311), respectively, as shown in Fig. 2a.

The size of crystallite is calculated using the Scherrer's Equation [8]

$$D = \frac{K\,\lambda}{\beta\,\text{Cos}\theta}, \tag{1}$$

where λ is the wavelength of the X-ray used in the characterisation, $K = 0.9$, β is the FWHM (Full Width at Half Maxima) of the sharp diffraction peak, and θ is the angle of diffraction. This equation is used to obtain the average size of the crystallite.

Since the graph of Pure PEDOT:PSS does not show any crystallinity; hence, the crystallite size of the pure sample could not be calculated. The crystallite size of nanocomposites ranged from approximately 34 nm through 43.5 nm to 45.5 nm for AgNPs-PEDOT:PSS 5%, AgNPs-PEDOT:PSS 10%, and AgNPs-PEDOT:PSS 15%,

Fig. 1 SEM images of Silver PEDOT:PSS nanocomposites with magnifications at **a** 1 µm, **b** 5 µm, and **c**, **d** 500 nm and **e** EDX mapping of the PEDOT:PSS-AgNPs nanocomposites
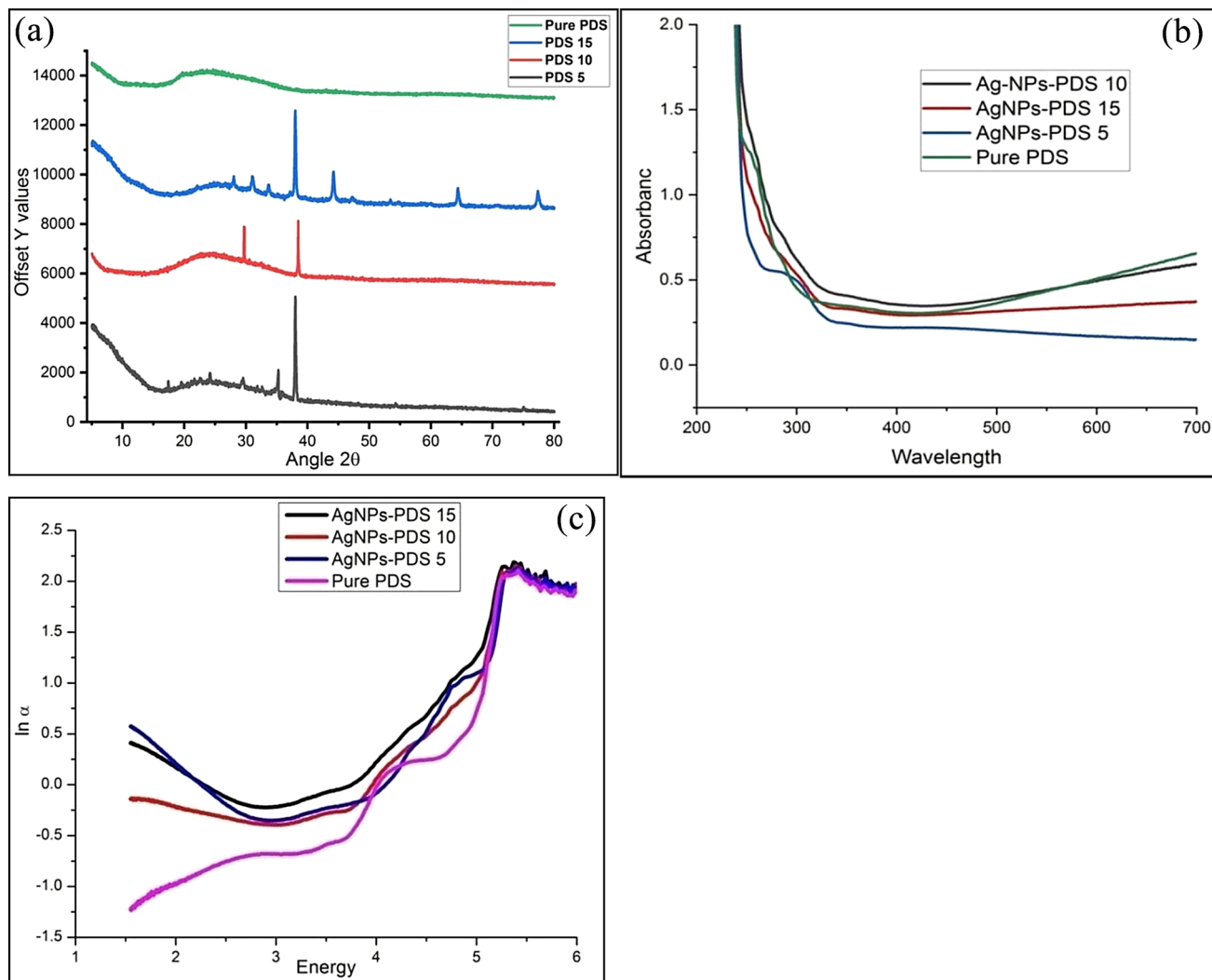
Fig. 2 a XRD graphs of Pure PDS, PDS 5%, PDS 10%, and PDS 15% showing characteristic peaks for Ag in mixed samples. **b** UV–Vis for Pure PDS, PEDOT:PSS-AgNPs 5%, PEDOT:PSS-AgNPs 10%, and PEDOT:PSS-AgNPs 15%. **c** Urbach plot for the as-prepared samples of Silver nanoparticles and PEDOT:PSS

respectively [9]. D-spacing calculated for the sharpest peak of all the samples at 2θ is calculated at 0.47 nm.

d-spacing between the planes of the crystal is calculated using Bragg's equation.

$$2d\mathrm{Sin}\theta = n\lambda,$$

where d is the spacing between the planes, n is the order of refraction, in this case, it is taken as 1, θ is the angle of incidence, and λ is the wavelength of X-ray. Microstrain is also calculated for the given crystallites at 6.93×10^{-4} using the equation.

$$\varepsilon = \frac{\beta_{hkl}}{4\tan\theta},$$

where β is the FWHM (Full Width at Half Maximum), ε is the microstrain, and θ is the glancing angle.

UV

Figure 2b shows the UV plot for the pure PEDOT:PSS, PEDOT:PSS-AgNPs 5%, PEDOT:PSS-AgNPs 10%, and PEDOT:PSS-AgNPs 15%. A little peak at 290 nm was observed for PEDOT:PSS, whereas for Silver nanoparticles mediated PEDOT:PSS also shows similar curves. Absorption for all the samples has been shifted towards higher wavelengths. Peaks for surface plasmon resonance have not been observed which could be due to the convolution of Silver nanoparticles into the matrix of PEDOT:PSS. Absorption of the curves could be traced to the composition spectra from increased π–π interaction amongst styrene components

of the sample. Such π–π interactions cause the delocalisation of electrons which results in the conduction of electrons in nanocomposites [10].

The relation between the absorption coefficient and band edge energy of photon is given by

$$\alpha = \alpha_0 \exp\left(h\nu/E_u\right),$$

where α_0 is a constant, h is the Planck's constant, ν is the frequency of the photon and the E_u is the width of localised states which is also known as Urbach energy. The Urbach energy for our nanocomposites has been calculated by taking the reciprocal of the intercept to the curve between ln and hν (Fig. 2c) [11]. Urbach energy calculated for the Pure PDS was 205meV; moreover, for PEDOT:PSS-AgNPs 5%, PEDOT:PSS-AgNPs 10%, PEDOT:PSS-AgNPs 15% were calculated 256, 288, and 353meV, respectively [12]. Increase in the Urbach energy with the rise in the concentration of

AgNPs (Silver nanoparticles) which further indicates an increase in defects in samples after the addition of AgNPs Silver nanoparticles. We could not calculate the Tauc plot energy for our results since they did not comply with the reported work.

CV

To examine the electrochemical properties of PEDOT: PSS and its nanocomposites, CV (Cyclic voltammetry) was carried out for working electrodes made of these nanocomposites coated on steel sheet with platinum counter electrode and Ag/AgCl reference electrode in 50-ml electrolyte of 1-M H_2SO_4 in the interval − 0.3 V to 0.7Vat the scan rate of 50mV/s. Cyclic voltammograms of Pure PEDOT:PSS, AgNPs-PEDOT:PSS 5%, AgNPs-PEDOT:PSS 10%, and AgNPs-PEDOT:PSS 15% are displayed in Fig. 3. Given voltammograms reveal a bulky curve for pure PEDOT:PSS
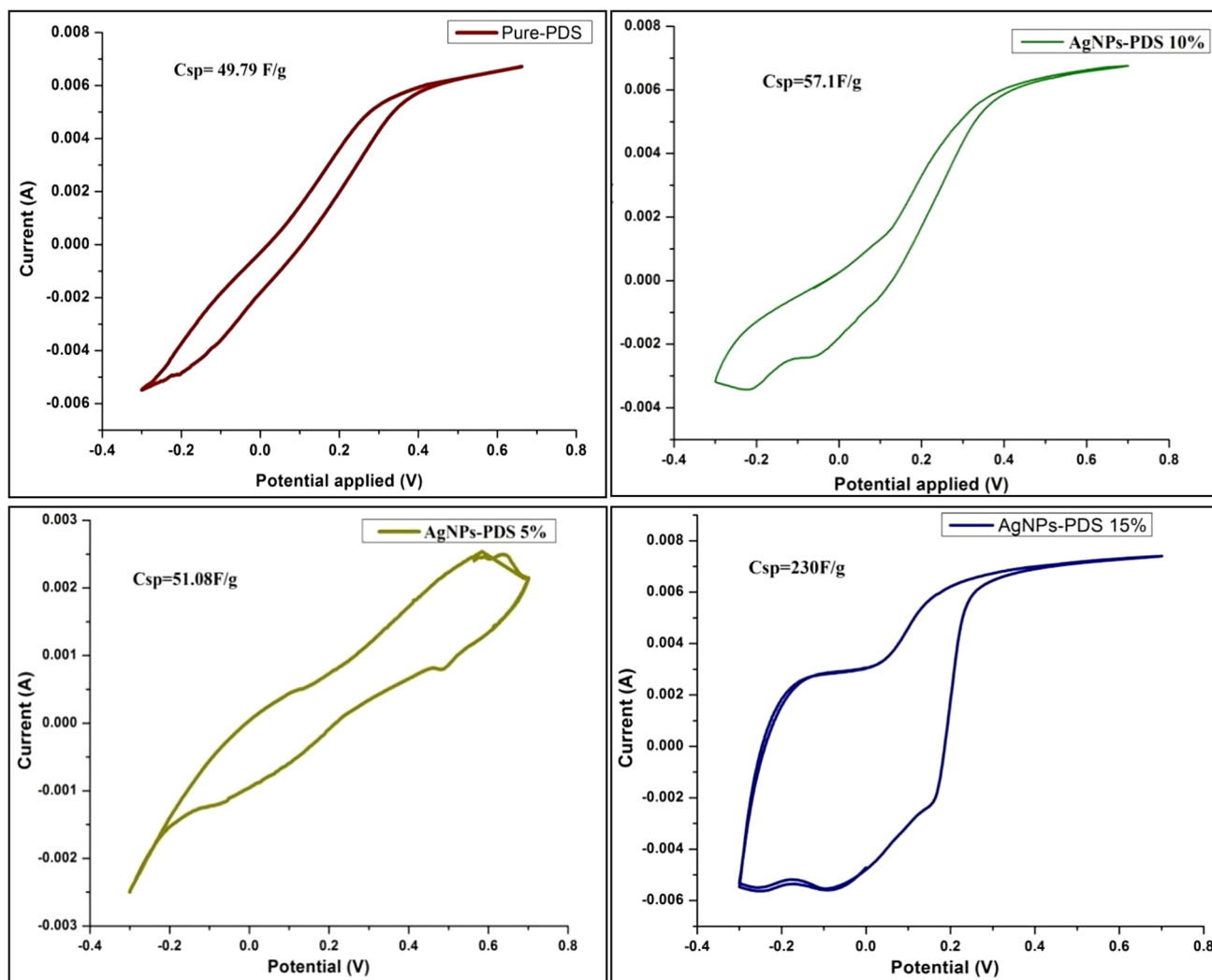

Fig. 3 Cyclic Voltammogram of Pure PDS, PDS-AgNPs 10%, PDS-AgNPs 5%, and PDS-AgNPs 15% at the scan rate of 50 mV/s

and thin wiry cycles for the doped samples revealing quasi-reversible redox voltammograms with partial symmetry showing inequitable cathode potential and anodic potential. Asymmetry of the curves can be attributed to the capacitance issues that may have arisen due to the IR drop of the large surface area of the electrode. From these graphs, specific capacitance is calculated using the following relation [13].

$$C_{sp} = \frac{\int_{V_a}^{V_b} Idv}{vm(V_b - V_a)},$$

where C_{sp} is the specific capacitance of the electrode, I is the current, m is the mass of the sample (0.5 mg), V_b and V_a are the potential limits of the voltage sweep, and v is the scan rate.

Electrochemical reaction of PEDOT:PSS is as follows [14]:

$$H_2SO_4 + PSS^- \rightarrow HSO_4^- + PSSH^+.$$
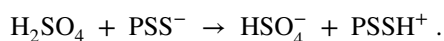
Reaction of Ag in H_2SO_4 is given as follows :

$$Ag^0 \leftrightarrow Ag^+ + e^-$$

Now the C_{sp} calculated using the above equation comes to be 51.08, 230.8, 57.1, and 49.79 F/g for AgNPs-PEDOT:PSS 5%, AgNPs-PEDOT:PSS 15%, AgNPs-PEDOT:PSS 10%, and Pure PEDOT:PSS, respectively, as observed in Fig. 3. It represents the improvement in the results discussed by Volkov et al. which could be ascribed to the porous structure of PEDOT:PSS electrode [15]. Similar results have been reported in literature for Ag-PEDOT:PSS composites [16]. An increase in specific capacitance is observed with the increase in concentration of AgNPs in PEDOT:PSS. Origin of capacitance in PEDOT:PSS can be explained by the stacking of ion-conducting PSS grains with the hole-conducting PEDOT chain. Layers are formed between electronically conducting PEDOT and the ionically conducting PSS to enable charge storage. AgNPs-PDS 15% showed improved specific capacitance because of synergism between AgNPs and PEDOT:PSS. This result when compared with results for other composites proved advantageous over the PEDOT–PSS:EG/rGO composite [17] which showed the specific capacitance of 174 F/g, whereas the specific capacitance of PEDOT:PSS/MWCNTs was reported 1314 F/g [5] which is much higher than the specific capacitance calculated in this study. Better specific capacitance of PEDOT:PSS/MWCNTs could be due to its excellent discharge properties.

Electron transfer in AgNPs-PEDOT:PSS may well be due to the movement of charges through metallic silver to the polymer PEDOT:PSS. π conjugation between PEDOT:PSS and AgNPs is increased and it leads to the structural disorder

Fig. 4 a Nyquist plot measured between 50 Hz for Pure PEDOT:PSS, ▶ AgNPs-PEDOT:PSS 5%, AgNPs-PEDOT:PSS 10%, and AgNPs-PEDOT:PSS 15%. **b** Bode plot for the EIS spectra for pure PEDOT:PSS, PEDOT:PSS-AgNPs 5%, PEDOT:PSS-AgNPs 10%, and PEDOT:PSS-AgNPs 15%

in PEDOT:PSS. AgNPs provide excess charge carriers to the surface of PEDOT:PSS thus providing a least resistance path for electrons.

EIS

Electrochemical Impedance spectroscopy (EIS) was used to study the electrochemical properties of AgNPs-PEDOT:PSS pellets. EIS was performed to obtain information about the interfacial electroactive species transfer kinetics. Figure 4a and b represents the Nyquist Plot and Bode plot for the observed values of the Pure PEDOT:PSS, AgNPs-PEDOT:PSS 5%, AgNPs-PEDOT:PSS 10%, and AgNPs-PEDOT:PSS 15%. Nyquist curves were fitted with an appropriate equivalent circuit that was analysed by Randall circuit model [18]. Figure 4c (exhibited in supplemental material) exhibits the high-frequency region for these Nyquist plots with very small semicircles that are the contributions from the bulk properties or grain boundaries in polymer PEDOT:PSS. Subsequent tail to the semicircle approaching the phase angle 45° could be attributed to the Warburg Phase element impedance at the lower end of the frequency signifying the formation of electron double layer [19].

All the samples studied in Nyquist plot have exhibited symmetric curves where we observed the drop in imaginary impedance Z" with decreasing amount of AgNPs in PEDOT:PSS polymer and fitted them with the circuit given below that contains Constant Phase element (CPE) Q_1, Q_2, and Q_3 with Bulk Resistance R_1, R_2, and R_3. Constant phase elements are used instead of Pure Capacitance in real systems because the actual capacitors do not give a pure semicircular pattern [20]. Hence, capacitance of the system in terms of impedance is given by

$$Z_{CPE} = \frac{1}{(jw)^\alpha Q},$$

where Z_{CPE} is the capacitance, j is the complex number, w is the angular frequency at the maximum of the imaginary point of Z'' in Nyquist plot, and Q is the parameter of Constant Phase Element (CPE) and is an empirical constant which is associated with the deviation of the plot from the vertical axis [21].

Spike at the lower end of the frequency signifies the formation of an electric double layer owing to the charge agglomeration at the electrode–electrolyte interface [22]. Real part of Impedance for curves of AgNPs-PEDOT:PSS 5% and
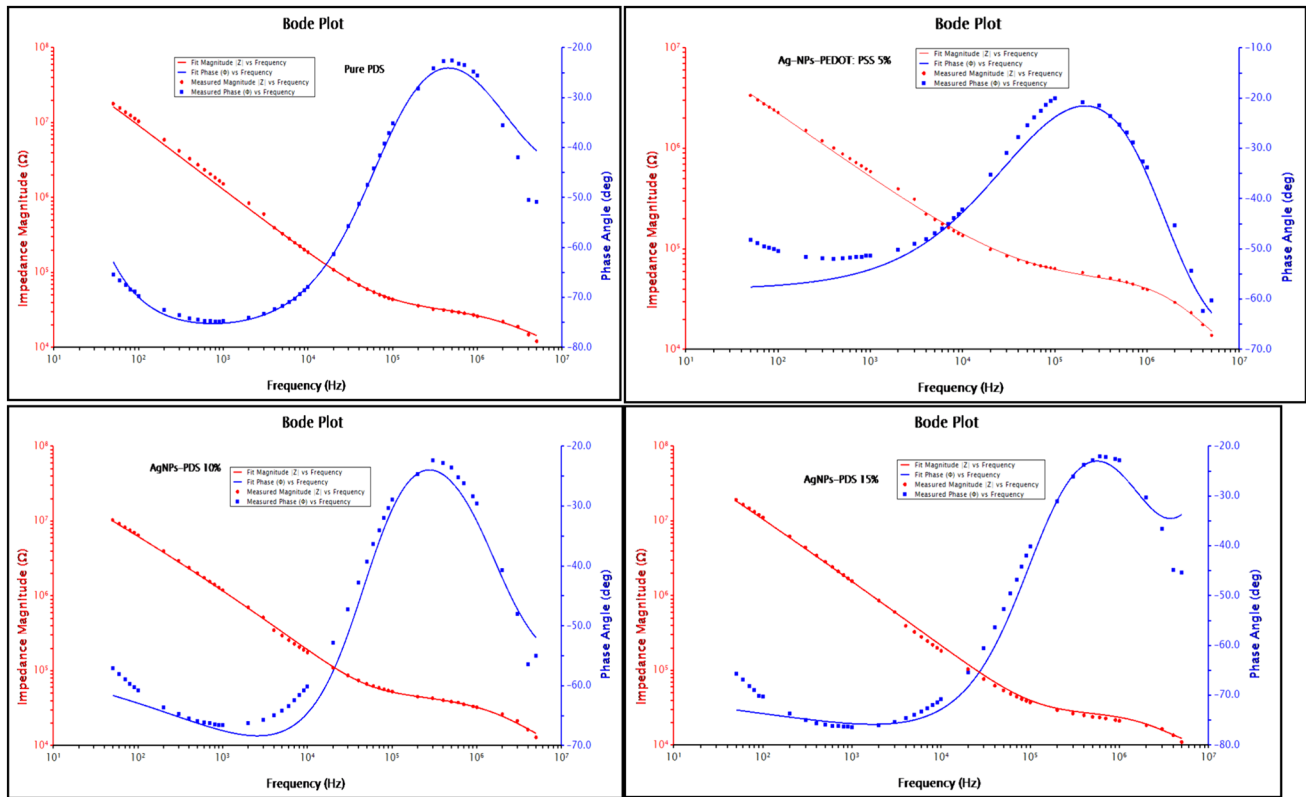
(a)
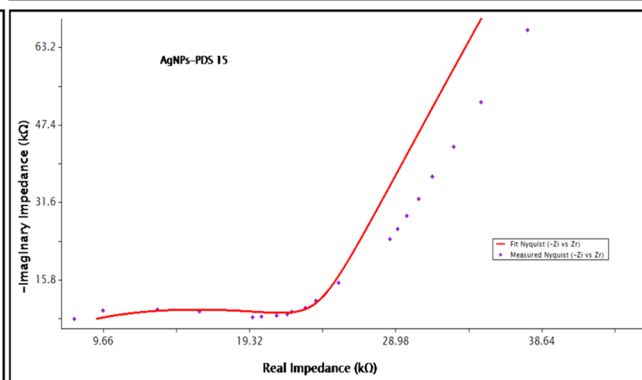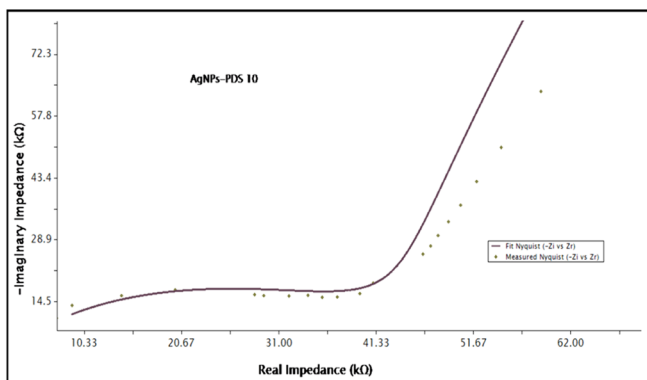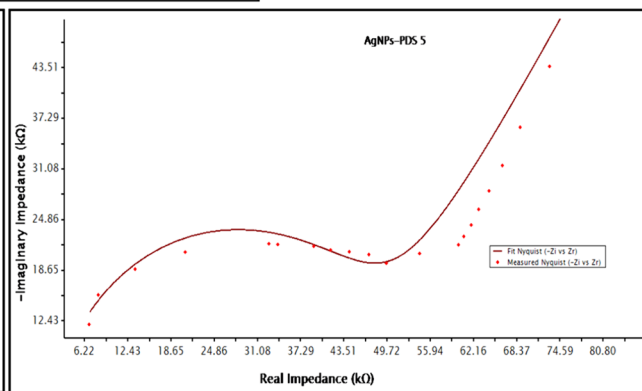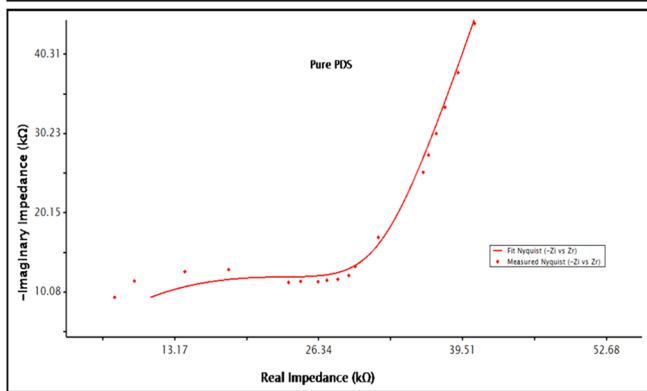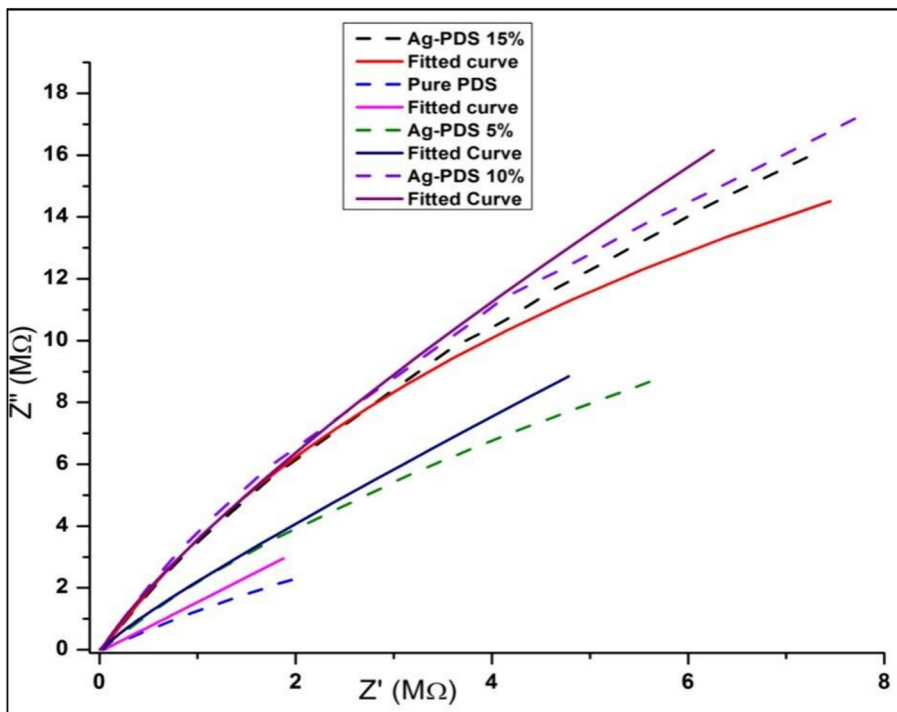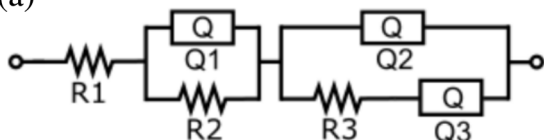
(b)

Fig. 4 (continued)

Table 1 Electrical parameters obtained with the help of circuit fitting of the Nyquist and Bode plot

	χ^2	Q1(Q (S/Ω) × 10^{-12}	Q1 (α)	Q2 (Q (S/Ω) × 10^{-12}	Q2 (α)	Q3 (Q (S/Ω) × 10^{-12}	Q3 (α)	R1 (Ω)	R2 (Ω)	R3 (Ω)	Ionic Conductivity (Mho/metre)
Pure PDS	0.194845	7.03	0.93474	1440	0.7648	10,600	0.5	1681.42	45613.5	41177	1.46×10^{-6}
Ag-PDS 5	0.244363	10	0.97082	2370	0.6078	103	0.947	0.01	14480.1	44559	4.6×10^{-6}
Ag-PDS 10	0.29627	12.9	0.91666	1220	0.5	209	0.9091	4165.91	19014.5	0.01	3.5×10^{-6}
PDS 15	0.491039	118	0.76656	4360	0.8572	42700	0.1780	2610.27	28705.3	994097	2.32×10^{-6}

χ = Chi value

Q1 = 1st Circuit Phase element

Q2 = 2nd Circuit Phase element

Q3 = 3rd Circuit Phase element

Q(α) = Corresponding Phase

AgNPs-PEDOT:PSS 10% do not vary significantly and hence their curves seem comparatively shorter. It indicates that these systems do not show significant activity at lower frequencies, whereas all the curves show satisfactory responses at higher wavelengths. Parameters fitted with the suitable circuit using the Aftermath software are given in Table 1 where Equivalent circuit of the model can be described as a parallel combination of Phase element Q_1 and Bulk resistance R_1 in series with another parallel combination of Q_2 with Resistance R_3 and Phase element Q_3 in series with one another [23].

It is noticed that the values of resistances R_1, R_2, and R_3 increase with the increasing addition of Silver nanoparticles.

The value of R_1 suddenly increases for the AgNPs-PEDOT:PSS 15%. It can also be attributed to the blocking of the electron transfer layer by excessive AgNPs. Circuit phase element for AgNPs-deposited pellets increases especially for AgNPs-PEDOT:PSS 15% which illustrates the formation of the metal-polymer layer that stores the charges. There is also an improvement in the speed of interfacial charge transfer of each electrode with the introduction of AgNPs in the polymer PEDOT:PSS [17].

Conclusion

Electrical effect of the incorporation of Silver nanoparticles in the Conducting polymer PEDOT:PSS has been studied. Various characterisations have been employed to measure the impact of AgNPs in the structural, electrical, and optical properties of the as-prepared AgNPs-PEDOT:PSS nanocomposites. Silver nanoparticles synthesised via green synthesis were incorporated in PEDOT:PSS with crystallite sizes ranging from 45 nm to 34 nm. Electrical properties were studied via CV and EIS spectroscopy. EIS was used to precisely characterise capacitance at small amplitudes and CV results agreed with results at the same amplitudes. Nyquist and Bode plots showed the electronic and ionic contribution towards the electrochemical activity of the sample. Calculated values of constant phase element and ionic conductivity showed significant rise with increasing silver nanoparticles content in PEDOT: PSS.

Moreover, other optical properties like Urbach energy and optical band gap were calculated using UV–Vis spectroscopy and Photoluminescence. The optical band gap was reduced with the introduction of Silver nanoparticles. Finally, this study shows that the incorporation of metallic nanoparticles in conducting polymers may prove fruitful in electrical storage and optoelectronic devices, e.g. Organic Batteries, Supercapacitors, and Organic Solar cells, owing to finer electronic and optical properties. For future, we would like to study the impact of PEDOT: PSS and other conducting polymers in this field by measuring the conductivity of the device made using these materials. Furthermore, incorporation of other metal nanoparticles like copper and gold and metal oxides could prove to be an intriguing work in this field.

Declarations

References

1. A.L. Pang, A. Arsad, M. Ahmadipour, Synthesis and factor affecting on the conductivity of polypyrrole: A short review. Polym. Adv. Technol. **32**, 1428–1454 (2020)
2. S. Bhandari, Polyaniline. Polyaniline Blends Compos. Nanocompos. (2018). https://doi.org/10.1016/B978-0-12-809551-5.00002-3
3. W.F. Quirós-Solano, N. Gaio, C. Silvestri, G. Pandraud, P.M. Sarro, PEDOT:PSS: a conductive and flexible polymer for sensor integration in organ-on-chip platforms. Procedia Eng. **168**, 1184–1187 (2016)
4. C. Wu, X. Zhou, J. Wei, Localized surface plasmon resonance of silver nanotriangles synthesized by a versatile solution reaction. Nanoscale Res. Lett. (2015). https://doi.org/10.1186/s11671-015-1058-1
5. N. Parveen, G.M. Alsulaim, S.A. Alsharif, H.H. Almutairi, H.A. Alali, S.A. Ansari, M.M. Ahmad, Renewable biopolymer-derived carbon–nickel oxide nanocomposite as an emerging electrode material for energy storage applications. J. Science: Adv. Mater. Devices. **8**, 100591 (2023)
6. S.A. Khan, S. Patel, P. Shukla, R. Kumar, R. Dixit, Synthesis and characterization of PVP embedded silver nanoparticles to study their structural and optical properties. J. Sci. Res. **66**, 139–143 (2022)
7. H.Y. Jeong, J.Y. Kim, T.H. Yoon, S.-Y. Choi, Bipolar resistive switching characteristics of poly(3,4-ethylene-dioxythiophene): Poly(styrenesulfonate) thin film. Curr. Appl. Phys. (2010). https://doi.org/10.1016/j.cap.2009.12.011
8. M.E. Yazdanshenas, M. Shateri-Khalilabad, The effect of alkali pre-treatment on formation and adsorption of silver nanoparticles on cotton surface. Fibers Polym. **13**, 1170–1178 (2012)
9. H.Z. Chi, Y. Li, Y. Xin, H. Qin, Boron-doped manganese dioxide for supercapacitors. Chem. Commun. **50**, 13349–13352 (2014)
10. A. Kuzmenko, (2018) Guide to ReffFIIT software to fit optical spectra
11. Y. Du, X. Cui, L. Li, H. Tian, W. Yu, Z. Zhou, Dielectric properties of DMSO-doped-pedot:PSS at Thz frequencies. Phys. Status Solidi (B) (2017). https://doi.org/10.1002/pssb.201700547
12. Y. Kim, J.-Y. Leem, Effects of precursor concentration on structural and optical properties of zno thin films grown on muscovite mica substrates by sol–gel spin-coating. J. Nanosci. Nanotechnol. **16**, 5186–5189 (2016)
13. T.-H. Meen, K.-L. Chen, Y.-H. Chen, W.-R. Chen, D.-W. Chou, W.-H. Lan, C.-J. Huang, The effects of dilute sulfuric acid on sheet resistance and transmittance in poly(3,4-thylenedioxythiophene): Poly(styrenesulfonate) films. Int. J. Photoenergy **2013**, 1–6 (2013)
14. B. Zhang, A.E. Jaouhari, X. Wu, W. Liu, J. Zhu, X. Liu, Synthesis and characterization of PEDOT-MC decorated agnps for

voltammetric detection of Rutin in real samples. J. Electroanal. Chem. **877**, 114632 (2020)

15. A.V. Volkov, K. Wijeratne, E. Mitraka, U. Ail, D. Zhao, K. Tybrandt, J.W. Andreasen, M. Berggren, X. Crispin, I.V. Zozoulenko, Understanding the capacitance of PEDOT:PSS. Adv. Funct. mater. (2017). https://doi.org/10.1002/adfm.201700329

16. S.R. Mohapatra, A.K. Thakur, R.N.P. Choudhary, Effect of nanoscopic confinement on improvement in ion conduction and stability properties of an intercalated polymer nanocomposite electrolyte for energy storage applications. J. Power Sources. **191**, 601–613 (2009)

17. J. Wu, Y. Deng, Y. Wu, L. Yan, Preparation of RGO/PEDOT:PSS composite with high photothermal conversion efficiency for light enhanced quasi-solid-state supercapacitor. J. Alloys Compd. **960**, 170463 (2023)

18. M. Naseri, L. Fotouhi, A. Ehsani, Nanostructured metal organic framework modified glassy carbon electrode as a high efficient non-enzymatic amperometric sensor for electrochemical detection of H2O2. J. Electrochem. Sci. Technol. **9**, 28–36 (2018)

19. I. Nuramdhani, A. Gokceoren, S. Odhiambo, De G. Mey, C. Hertleer, Van L. Langenhove, Electrochemical impedance analysis of a PEDOT:PSS-based Textile Energy Storage device. Materials. **11**, 48 (2017)

20. S.B. Aziz, Z.H. Abidin, A.K. Arof, Influence of silver ion reduction on electrical modulus parameters of solid polymer electrolyte based on chitosan-silver triflate electrolyte membrane. Express Polym. Lett. **4**, 300–310 (2010)

21. A. Iwan, B. Boharewicz, I. Tazbir, A. Sikora, B. Zboromirska-Wnukiewicz, Silver nanoparticles in pedot: PSS layer for polymer solar cell application. Int. J. Photoenergy **2015**, 1–9 (2015)

22. D. Pang, C. Ma, D. Chen, Y. Shen, W. Zhu, J. Gao, H. Song, X. Zhang, S. Zhang, Silver nanoparticle-functionalized poly (3, 4-ethylenedioxythiophene): polystyrene film on glass substrate for electrochemical determination of Nitrite. Org. Electron. **75**, 105374 (2019)

23. J.Y. Kim, J.H. Jung, D.E. Lee, J. Joo, Enhancement of electrical conductivity of poly(3,4-ethylenedioxythiophene)/poly(4-styrenesulfonate) by a change of solvents. Synth. Met. **126**, 311–316 (2002)